

Myofascial force transmission is increasingly important at lower forces: firing frequency-related length–force characteristics of rat extensor digitorum longus

H. J. M. Meijer,¹ G. C. Baan¹ and P. A. Huijting^{1,2}

¹ Instituut voor Fundamentele en Klinische Bewegingswetenschappen, Faculteit Bewegingswetenschappen, Vrije Universiteit, Amsterdam, The Netherlands

² Integrated Biomechanical Engineering for Restoration of Human Function, Instituut voor Biomedische Technologie, Faculteit Werktuigbouwkunde, Universiteit Twente, Enschede, The Netherlands

Received 20 May 2005,
revision requested 30 June 2005,
revision received 31 October
2005,
accepted 25 November 2005
Correspondence: H. J. M. Meijer,
Instituut voor Fundamentele en
Klinische
Bewegingswetenschappen,
Faculteit
Bewegingswetenschappen, Vrije
Universiteit, van der
Boechorststraat 9, 1081 BT
Amsterdam, The Netherlands.
E-mail: h.meijer@fbw.vu.nl

Abstract

Aim: Effects of submaximal stimulation frequencies on myofascial force transmission were investigated for rat anterior crural muscles with all motor units activated.

Methods: Tibialis anterior and extensor hallucis longus (TAEHL) muscles were kept at constant muscle–tendon complex length, but extensor digitorum longus muscle (EDL) was lengthened distally. All muscles were activated simultaneously at 10, 20, 30 and 100 Hz within an intact anterior crural compartment.

Results: At lower frequencies, significant proximo-distal EDL force differences exist. Absolute EDL proximo-distal active force differences were highest at 100 Hz ($\Delta F_{\text{dist-prox}} = 0.4$ N). However, the normalized difference was highest at 10 Hz ($\Delta F_{\text{dist-prox}} = 30\% F_{\text{dist}}$). Firing-frequency dependent shifts of the ascending limb of the EDL length–force curve to higher lengths were confirmed for a muscle within an intact compartment, although effects of firing frequency assessed at proximal and distal EDL tendons differed quantitatively. As EDL was lengthened distally, TAEHL distal isometric active force decreased progressively. The absolute decrease was highest for 100 Hz ($\Delta F_{\text{from initial}} = -0.25$ N). However, the highest normalized decrease was found for 10 Hz stimulation ($\Delta F_{\text{from initial}} = -40\%$).

Conclusions: At submaximal stimulation frequencies, myofascial force transmission is present and the fraction of force transmitted myofascially increases with progressively lower firing frequencies. Evidently, the stiffness of epimuscular myofascial paths of force transmission decreases less than the stiffness of serial sarcomeres and myotendinous pathways. It is concluded that low firing frequencies as encountered *in vivo* enhance the relative importance of epimuscular myofascial force transmission with respect to myotendinous force transmission.

Keywords anterior crural compartment, connective tissue, extensor digitorum longus muscle, firing frequency, length force characteristics, myofascial force transmission, tibialis anterior muscle.

In addition to myotendinous force transmission (Trotter *et al.* 1985, Tidball 1991, Trotter 2002), force exerted by sarcomeres is transmitted via alternative pathways (Street & Ramsey 1965, Street 1983). Via the muscle fibre cytoskeleton, which is connected to the basal lamina, a fraction of the force exerted by sarcomeres is transmitted onto the connective tissue within the muscle (myofascial force transmission). This intramuscular connective tissue is connected to the intermuscular connective tissues and to similar stromata of other muscles as well as to extramuscular connective tissues. Proof of the existence of such epimuscular myofascial force transmission is a difference in force exerted at the origin and insertion of a muscle (Huijing 1998, Huijing & Baan 2001a, 2003). Such transmission has been shown for muscles within the anterior crural compartment of the rat (Huijing & Baan 2001a,b), and in gradually dissected rat medial gastrocnemius muscle (Rijkelijhuizen *et al.* 2005), the rat flexor carpi ulnaris (FCU) muscle (Smeulders *et al.* 2002) as well as human FCU in patients with cerebral palsy (Kreulen *et al.* 2003, 2004). One of the important factors affecting muscle length–force characteristics is the level of muscular excitation. The effects of stimulation frequencies on muscle length–force characteristics, of fully dissected *in situ* muscles, have been recognized since the observations of Rack & Westbury (1969): at low stimulation frequencies, the length–force curves of muscles are not scaled versions of their curves at 100 Hz. Using pulse trains with a constant asynchronous stimulation frequency (CSF), it was shown that the ascending limb of the length–force curve of cat soleus muscle shifted to higher muscle length as stimulation frequency was lowered (Rack & Westbury 1969, Roszek & Huijing 1997, Brown *et al.* 1999).

The major mechanisms by which length–force characteristics are altered are predominantly intracellular ones, such as the length-dependent calcium sensitivity of force; increasing sarcomere length results in an enhanced sensitivity to calcium (Stephenson & Williams 1982, Stephenson & Wendt 1984). The question arises whether such effects, of intracellular origin, on length–force characteristics are recognizable also in muscle that is still embedded within its natural context of connective tissues, or that such effects are modified by higher levels of tissue organization [as argued as a possibility by Huijing (2003) and Huijing & Jaspers (2005)]. Major distributions in sarcomere lengths due to myofascial force transmission (Yucesoy *et al.* 2002, Maas *et al.* 2003a) could be a factor in such potential modifications. Low muscular firing frequencies play an important role in the *in vivo* motor control. For example, firing frequencies in rat muscle vary between 10 and 60 Hz (Hennig & Lomo 1985). Therefore, it is necessary to assess the presence and importance of epimuscular

myofascial force transmission at physiological stimulation frequencies. This thought is also inspired by work by Kronecker & Cash (1880), who, after noting effects of a passive muscle on an actively shortening neighbouring muscle, reported that at intermediate levels of stimulation of the muscle, the neighbouring active muscle was not impeded significantly. This may suggest that although myofascial force transmission is highly important at maximal stimulation, this may not be the case at submaximal levels of stimulation. Therefore, the aim of this study is twofold: (1) to assess the presence of epimuscular myofascial force transmission at low firing frequencies, and if present at significant levels, its relative importance compared with that at high firing frequencies; and (2) if present, to assess if myofascial force transmission modifies the firing frequency-related effects on muscle length–force characteristics.

Methods

Surgical and experimental procedures were in agreement with the guidelines and regulations concerning animal welfare and experimentation set forth by Dutch law, and approved by the Committee on Ethics of Animal Experimentation at the Vrije Universiteit. Immediately after all experiments, animals were killed using an overdose of urethane solution, and double-sided pneumothorax was performed.

Surgical procedures

Seven male Wistar rats [*Rattus norvegicus* (Berkenhout, 1769)] with a mean body mass of 303.4 g (SD = 11.80) were anaesthetized using intraperitoneally injected urethane solution (1.5 g kg⁻¹ body mass). Extra doses were given if necessary (maximally 1.5 mL). During surgery and data collection, the rats were placed on a heated water pad of approx. 37 °C, to prevent hypothermia.

The anterior crural compartment, which envelopes tibialis anterior (TA), extensor digitorum longus (EDL) and extensor hallucis longus (EHL) muscles (see Fig. 1), was exposed by removing the skin and most of the biceps femoris muscle from the left hind limb. Connective tissue at the muscle bellies of TA, EHL and EDL was left intact. However, the transverse crural ligament and the crural cruciate ligament were severed and limited fasciotomy was performed to dissect the distal tendons of EDL, TA and EHL. As it is difficult to measure force exerted by each EDL tendon individually, without friction between neighbouring tendons, the four EDL tendons were tied together using polyester thread. For the same reasons, the distal tendons of TA and EHL as well as the distal tendons of peroneal muscles (PER) were tied to each other, creating a

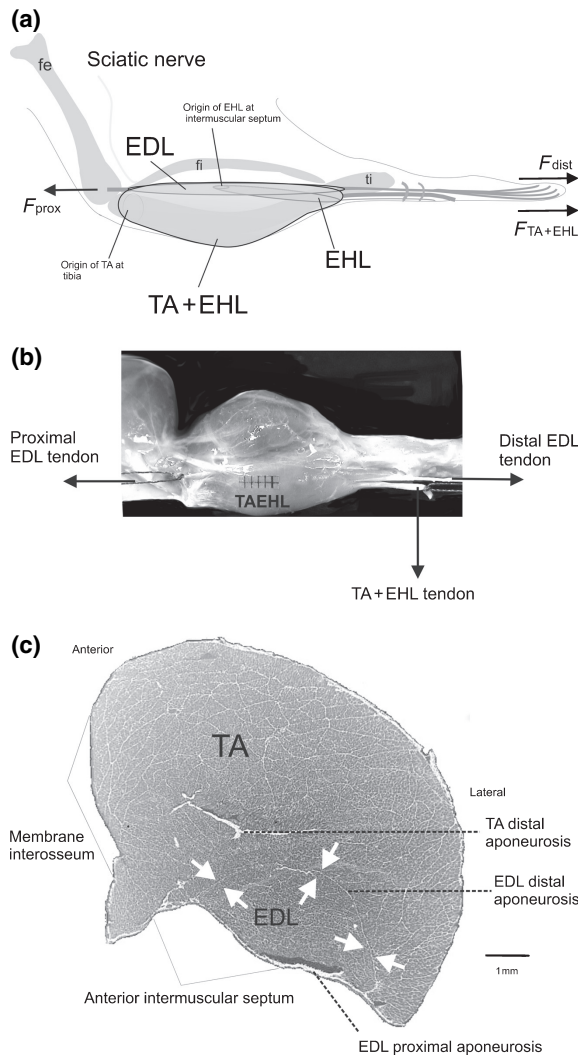


Figure 1 Representation of the experimental set up and muscle anatomy of the rat anterior crural compartment. (a) Schematic lateral view of the rat anterior crural compartment after removal of the skin and biceps femoris muscle. Connective tissue at the muscle bellies was left intact. Origins and insertions of muscles are shown. Proximally, the extensor digitorum longus (EDL) tendon attaches at the lateral condyle of the femur and the tibialis anterior (TA) originates from the antero-proximal face of the tibia. The TA + EHL complex is made transparent in the image to allow showing of the position of the EDL and the EHL originating at the anterior intermuscular septum. The distal tendons of EDL insert on the four toes. Both distal TA and EHL tendons curve medially to insert on metatarsal I. The proximal EDL tendon was severed and attached to a force transducer using a metal rod (represented by an arrow). Distally, the tendons of EDL as well as of the TA + EHL complex were connected to separate force transducers using metal rods (represented by arrows). Both tibia and foot were fixed within a rigid frame so that the muscles were aligned with the force transducers. (b) Lateral view of gross muscle anatomy after removal of the skin and biceps femoris muscle. After limited fasciotomy, the distal and proximal tendon of EDL and the distal tendon of TA + EHL were severed. EDL muscle is covered completely by TA + EHL muscle and GM muscle, except for both proximal and distal tendons. (c) Inverted image of a cross-section of the rat anterior crural compartment at 50% of the proximo-distal length of the EDL muscle belly, showing TA muscle enveloping a large part of EDL. The EHL is only present more distally. The TA–EDL connective tissue interface is indicated by white arrows. Bar indicates 1 mm.

complex of these muscles. Two pieces of the epicondylus lateralis of the femur were cut, representing the origin of EDL muscle and of the lateral collateral ligament. Both pieces of bone were attached to metal rods using 100% polyester yarn. Markers were placed on the gastrocnemius muscle, representing the original proximo-distal position of the origin of the EDL muscle and lateral collateral ligament. Screws were inserted into the medial surface of the tibia and used for tibia fixation. The foot was firmly fixed to a plate. Both tibia and footplate were fixed within a rigid frame in such a way that the muscles were aligned with the force transducer. Within the femoral compartment, the tibial nerve and the sural branch of the sciatic nerve were cut as proximally as possible. The sciatic nerve was dissected free of its surroundings. Only the peroneus communis nerve branch was left intact, other branches were denervated. Branches of the intact common peroneal nerve innervate EDL, TA and EHL muscles. Stimulation of the nerve will, therefore, activate all three muscles simultaneously.

The experimental apparatus

The rat was placed on a platform. The footplate was positioned in such a way that the ankle angle was in extreme plantar flexion to make room for free passage of the distal tendons (Fig. 1). The knee was kept at a 110° angle. All three distal tendon complexes as well as the proximal EDL tendon and the collateral lateral ligament (the latter two still attached to pieces of bone) were connected to force transducers (BLH Electronica, Canton, MA, USA; maximal output error <0.1%, compliance of 0.0162 mm N⁻¹) using stainless steel rods to ensure isometric contractions. The force transducers were mounted on single axis micropositioners. The sciatic nerve was placed in a pair of electrodes (supramaximal current).

Experimental conditions

The nerve was prevented from dehydration by covering it with paper tissue saturated with isotonic saline and covered by a thin piece of latex. Ambient temperature (22 °C ± 0.5 °C) and air humidity (70 ± 2%) were kept constant by a computer controlled air-conditioning system (Holland Heating, Waalwijk, the Netherlands).

Muscle and tendon tissue was further prevented from dehydration by regularly irrigating the tissue with isotonic saline. Timing of stimulation of the nerve and A/D conversion (12-bit A/D converter, sampling frequency 1000 Hz, resolution of force 0.01 N) were controlled by a special purpose microcomputer. Before each contraction, the EDL muscle was brought to the desired length passively by moving the distal force transducer exclusively. The tibialis anterior and extensor hallucis longus (TAEHL) complex and the peronei muscles were kept at constant length set to exert an initial force of respectively 3 and 5 N. The collateral lateral ligament was kept at a position equivalent to its *in situ* position corresponding to the knee angle imposed. The original proximal EDL position was determined by using the corresponding marker position on the gastrocnemius muscle. The proximal EDL position was subsequently placed at a length which was 2 mm shorter than the original marker position. The experimental stimulation protocol consisted of two twitches (at $t = 200$ and $t = 400$ ms), followed by a pulse train (at $t = 600$ ms) with a staircase complex of ascending stimulation frequencies (ASF) of 10, 20, 30 and 100 Hz (Fig. 2), and a final twitch at $t = 1800$ ms. The successive pulse frequency phases were equal in duration (250 ms) and total stimulation time was 1000 ms. After each contraction, the muscles were allowed to recover near active slack length for 2 min. Before acquiring data, EDL muscle was preconditioned by isometric contractions alternatively at high and low lengths of EDL until forces at low length were reproducible, i.e. effects of previous activity at high lengths are removed (Huijing & Baan 2001a,b). Isometric contractions were performed at different EDL lengths starting near muscle active slack (i.e. the smallest muscle length at which muscle active force approaches zero). The muscle–tendon complex was distally lengthened with 1.0 mm increments. Results are plotted for a length range to 3 mm over 100 Hz optimum length. Passive isometric muscle force was measured just prior

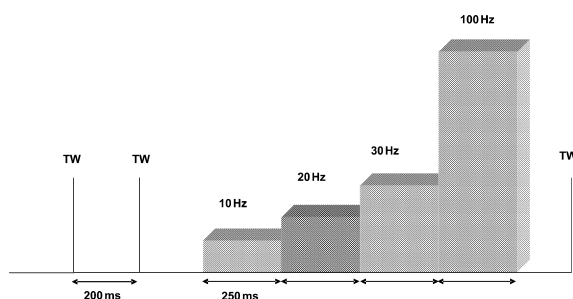


Figure 2 Schematic representation of the ascending stimulation frequency (ASF) protocol. The protocol started with two twitches (TW), followed by an ascending staircase of 10, 20, 30 and 100 Hz stimulation, and ended by a twitch.

to the tetanic contraction, and total isometric muscle force was measured during the tetanic plateau of the muscle force.

Treatment of data and statistics

Passive muscle force was fitted using an exponential curve $y = \exp(ax + b)$, where y represents passive muscle force, x represents muscle length and 'a' and 'b' are fitting constants. Active EDL muscle force (F_{ma}) was estimated by subtracting passive force (F_{mp}) for the appropriate muscle length from total force (F_m). Active EDL length–force data were then fitted with a stepwise polynomial regression procedure. In this procedure, the curve fit is determined by increasing the order (maximum of 6) of the polynomial as long as this yields a significant improvement to the description of the length–active force data, as determined by one-way analysis of variance (ANOVA). The polynomial: $y = b_0 + b_1x + b_2x^2 + \dots + b_nx^n$, where y represents active muscle force, x represents active muscle force length and $b_0 \dots b_n$ are fitting constants. Optimum muscle length was defined for each curve as the active muscle length at which the fitted curve showed maximal active muscle force (F_{mao}). Using the selected polynomials, mean and SE of active muscle force were calculated for a given EDL length. In order to estimate more accurately the distal active slack length, data of muscle length and active muscle force ($F_{ma} < 0.3 \times F_{mao}$) were selected. The data points were then extrapolated with a fitted curve where $y = \exp(b_0x + b_1) + b_2$. Active slack length was determined by solving the roots for this equation. Two-way ANOVA's for repeated measures were performed to test for the effects of stimulation frequency (four levels: 10, 20, 30 and 100 Hz) and EDL muscle length on the force exerted at the proximal and distal tendons of EDL muscle as well as TAEHL complex forces. In addition, a two-way ANOVA was used to test for the effects of stimulation frequency and EDL muscle length on the distally and proximally measured optimum muscle length (L_{mao}). To test for the presence of a proximo-distal EDL force difference, one-way ANOVA was performed. If significant effects were found, *post-hoc* tests were performed using the Bonferroni procedure for multiple pairwise comparisons to locate differences. Main and interaction effects as well as differences were considered significant at $P < 0.05$.

Results

Effects of stimulation frequency on length–force characteristics of EDL muscle

Representative time – EDL force traces of the ascending frequency stimulation protocol are shown in Figure 3.

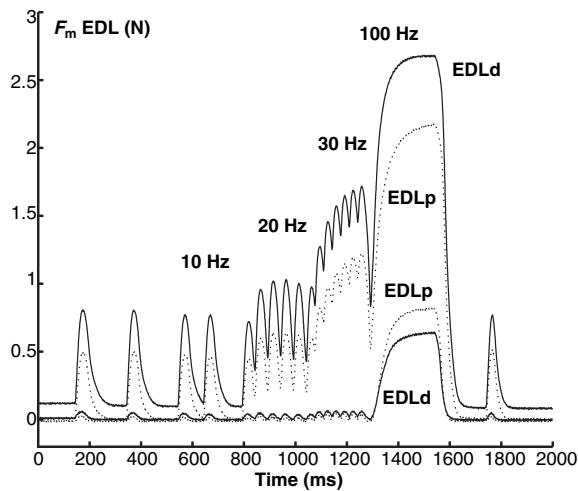


Figure 3 Representative proximal and distal time-force traces obtained by applying the ascending frequency stimulation protocol. Near active slack length (lower traces); near optimum muscle length (upper traces). ‘EDLd’ indicates distal EDL force; ‘EDLp’ indicates proximal EDL force.

The protocol started with two twitches followed by 10 Hz stimulation. In three steps, the stimulation frequency was increased to 100 Hz and EDL force increases with it. Note that at low as well as at high muscle length, the tetani are not completely fused for stimulation frequencies of 10–30 Hz. At low muscle length, EDL forces are low. Note that EDL proximal force is higher than EDL distal force. Both forces reach the plateau phase simultaneously. At higher muscle length, EDL distal force reaches the tetanus plateau earlier than EDL proximal force. EDL distal force is now higher than EDL proximal force.

For distal EDL active force, ANOVA indicates significant main effects of stimulation frequency and EDL length as well as an interaction between these factors (Fig. 4a). The ascending frequency protocol (ASF) was attended by significantly higher muscles force. Force enhancement was length dependent ($P < 0.05$) and force decreased at muscle lengths over the optimum length. Distal active force increases with increasing length in two major ways: (1) a flatter region; the length range from active slack length to $\Delta l_{m+t} \approx -7$ to -8 ; and (2) a steeper region; the length range between $\Delta l_{m+t} \approx -7$ and optimum lengths. No significant shifts of distal active slack lengths (estimated by extrapolation) could be shown. Extrapolation to zero force of proximal length–force data was unreasonable because of high levels of proximal force remaining as well as the shape of the curve. For lower frequencies, optimum muscle length shifted substantially to higher muscle length (e.g. for 10 Hz the shift equalled 2.4 mm, see Fig. 5b). Distal passive force increased exponentially as a function of EDL muscle length. Note that a rise in passive force starts well below optimum length (i.e.

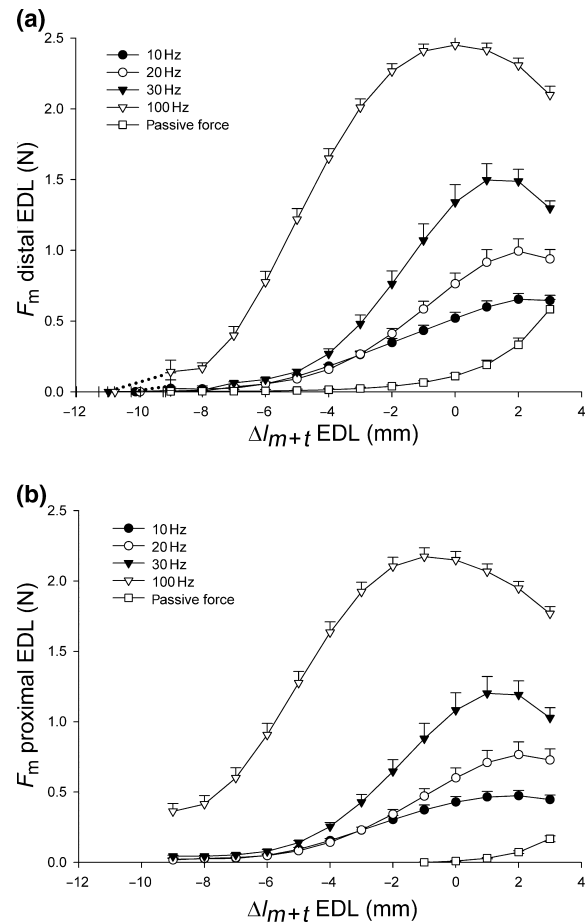


Figure 4 Effects of firing frequency on extensor digitorum longus (EDL) length–force characteristics. All values are shown as means + SE, $n = 6$. (a) Length–force characteristics as measured at the distal tendon. (b) Length–force characteristics as measured at the proximal tendon. EDL length, increased by distal EDL lengthening (Δl_{m+t} EDL dist), is expressed as deviation from distal optimum length for 100 Hz stimulation.

$\Delta l_{m+t} \approx -5$). For proximal active force (Fig. 4b), ANOVA indicates significant effects of stimulation frequency and muscle length as well as an interaction between these factors. Proximal active force also increased as a function of EDL muscle length in two phases, but the length ranges seem different from those of distal EDL active force: for the lower stimulation frequencies, the slower increase ends at higher lengths (i.e. $-6 < \Delta l_{m+t} < -5$) but for 100 Hz this phase ends at lower lengths ($\Delta l_{m+t} \approx -8$). At lower stimulation frequencies, optimum muscle length of proximal active force was shown to have shifted significantly to higher lengths (e.g. 2.6 mm at 10 Hz stimulation, see Fig. 5b). Proximal passive force increased exponentially with lengthening of EDL. Note that proximal passive force does not increase substantially until optimum length is attained.

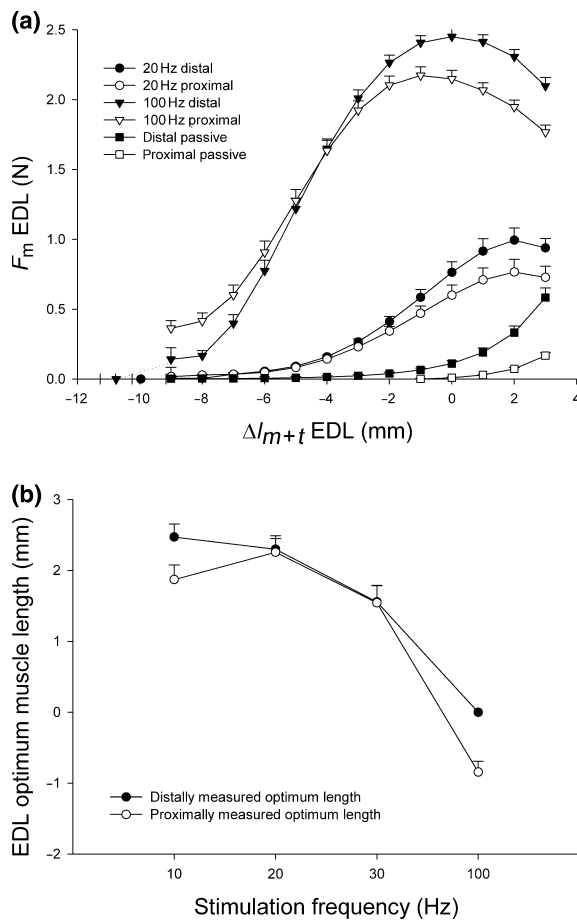


Figure 5 Comparison of extensor digitorum longus (EDL) proximal and distal length force characteristics at different stimulation frequencies. All values are shown as means + SE, $n = 6$. (a) Length–force characteristics of EDL muscle–tendon complex length, increased by distal EDL lengthening (Δl_{m+t} EDL dist), expressed as deviation from 100 Hz distal optimum length. (b) Proximal and distal optimum muscle lengths (l_{mao}) vs. stimulation frequency.

Proximo-distal EDL force differences and effects of stimulation frequency

Figure 5a shows examples of the length–force curves of EDL proximal and distal active force at 20 and 100 Hz stimulation. Proximal and distal EDL active forces differ as a function of muscle–tendon complex lengths and stimulation frequency. Note that distal EDL passive force is also significantly higher than proximally measured EDL passive force. For 10 and 100 Hz stimulation frequency, optimum length measured at the proximal tendon of EDL differs from optimum length measured at the distal tendon (Fig. 5b), but not for 20 and 30 Hz stimulation.

A plot of proximo-distal force differences (Fig. 6a) shows that except for 100 Hz stimulation, proximal and distal active forces are similar at low muscle lengths

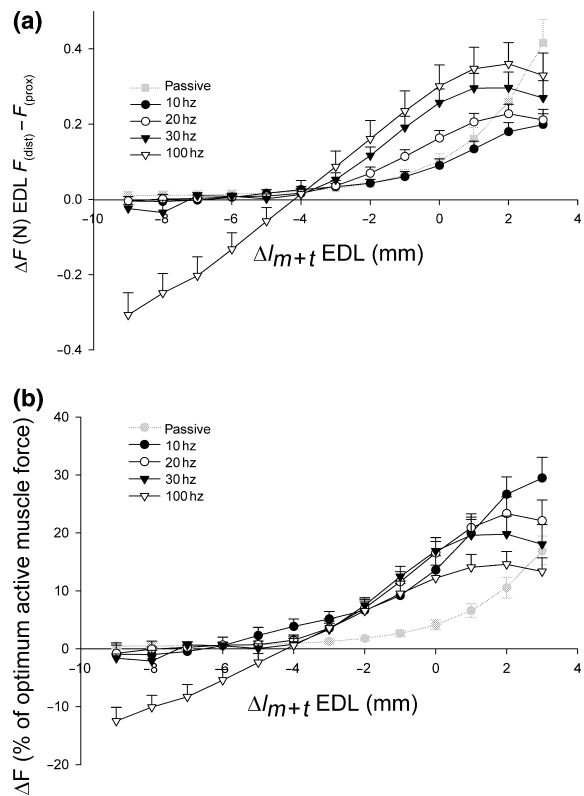


Figure 6 Effects of stimulation frequency and extensor digitorum longus (EDL) muscle tendon complex length, increased by distal EDL lengthening (Δl_{m+t} EDL dist), on the proximo-distal force difference. Values are shown as means + SE, $n = 6$. (a) ΔF , absolute difference between distal and proximal active and passive force. (b) ΔF , normalized for distal optimum active force per frequency [F_{mao} (f)] and passive force (normalized for distal 100 Hz optimum force). Both graphs are plotted as a function of muscle–tendon complex length (Δl_{m+t}) of EDL. EDL muscle–tendon complex length is expressed as a deviation from 100 Hz distal optimum length.

($-9 < l_{m+t} < -5$). However, for $l_{m+t} > -5$, distal active force is dominant over proximal active force. The proximo-distal EDL active force difference increased until well over optimum length (Fig. 6a). The absolute difference in active force between the proximal and distal tendon is highest for 100 Hz stimulation ($\Delta F = 0.36$ N), and is lowest at 10 Hz stimulation ($\Delta F = 0.2$ N). At low muscle lengths, ($-9 < l_{m+t} < -5$), proximal and distal passive forces are equal. The passive proximo-distal force difference starts to increase exponentially for $l_{m+t} > -5$ and eventually becomes larger than the active proximo-distal force difference.

In contrast, for a certain length range ($-3 < \Delta l_{m+t} < 0$) force differences, normalized for distal optimum force per frequency, are quite similar for different stimulation frequencies (Fig. 6b). For other length ranges, substantial differences were found. At higher lengths, 10 Hz stimulation caused the highest

normalized difference (up to 30% F_{mao}) and 100 Hz stimulation the lowest (up to $\pm 15\%$ F_{mao}). At low lengths, only major normalized proximo-distal force differences were found for 100 Hz (-20%) stimulation. The normalized passive force difference equals zero at low muscle lengths, but shows an exponential increase at $l_{m+t} > -5$. The increase of a significant proximo-distal force difference with lower stimulation frequencies, suggest that the transmission of force by epimuscular myofascial pathways increases relatively with respect to myotendinous force transmission at low frequency stimulation.

Effects of EDL length and stimulation frequency on TAEHL complex force

ANOVA showed significant main effects of EDL muscle–tendon complex length and stimulation frequency on TAEHL active force as well as an interaction between these factors, on TAEHL active force (Fig. 7). TAEHL active force increased significantly with firing frequency. Distal lengthening of the EDL muscle–tendon complex caused the TAEHL active force to decrease significantly despite the fact that TAEHL muscle–tendon complex length was left unchanged. Figure 7b shows that the decreases in force normalized for the initial levels are substantial (e.g. 10 Hz active force dropped approx. 40%). Note that normalized force decrease is lowest for 100 Hz and highest for 10 Hz. Note also that decreasing TAEHL active force coincides with increasing EDL proximo-distal active force difference, particularly at higher lengths. This is taken as an indication that, as EDL is lengthened, at least part of TAEHL active force is exerted at the distal tendon of EDL through myofascial pathways.

Discussion

EDL proximo-distal force differences and myofascial force transmission

At submaximal firing frequencies, isometric force exerted at the proximal and distal tendons of EDL muscle was found to differ as a function of EDL length. These findings are in agreement with those of previous studies on epimuscular myofascial force transmission in maximally activated muscle (Huijing *et al.* 1998, Maas *et al.* 2001). Any such proximo-distal force difference indicates that net forces, additional to myotendinous ones, act as a load on the muscle. Intact inter- and/or extramuscular connections surrounding the EDL muscle mediate this myofascial force transmission (Huijing & Baan 2001a). The effects of such force transmission do not arise from innate characteristics of the muscle fibre, but can be best understood on the basis of changes in

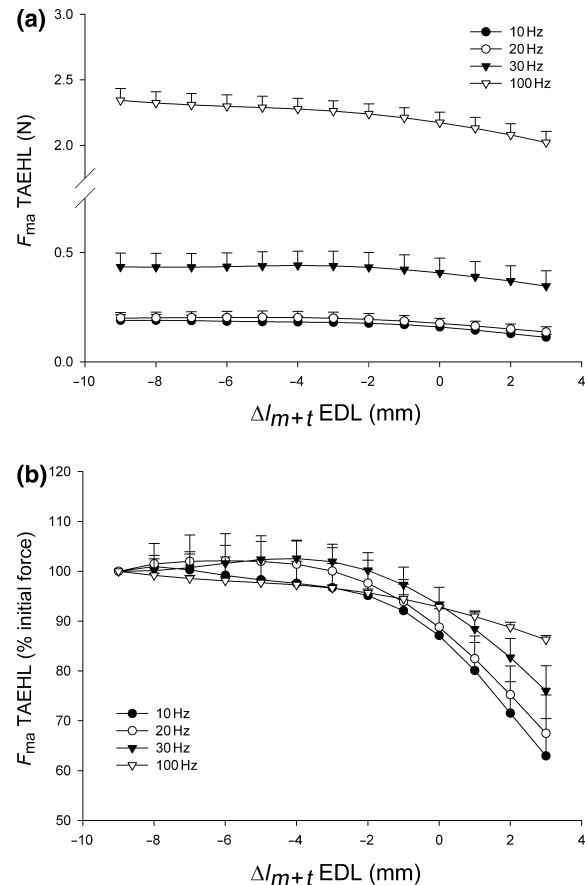


Figure 7 Effects of distal extensor digitorum longus (EDL) lengthening (Δl_{m+t} EDL dist) on tibialis anterior (TA) + EHL forces. Values are shown as means + SE, $n = 6$. (a) TA + EHL active forces; (b) TAEHL active forces expressed as a percentage of the initial active force. Both graphs are plotted as a function of EDL muscle–tendon complex length (Δl_{m+t} EDL dist). EDL muscle–tendon complex length is expressed as a deviation from 100 Hz distal optimum length.

length, direction of applied length changes, as well as relative positions of muscles and concomitant changes in the configuration of extra- and intermuscular connective tissues connecting EDL and the TA + EHL complex (Huijing & Baan 2001a, Maas *et al.* 2003b). It indicates that, when considering a muscle active within an intact organism, an integrative approach is needed (Huijing 2003), which also accounts for changes in muscle characteristics as a result of interaction with tissues at higher levels of organization.

The decrease in active force exerted by TAEHL while kept at constant muscle tendon complex length (Fig. 7a), can be seen as a direct effect of epimuscular myofascial force transmission due to changes in the configuration of the connective tissue between EDL and TA + EHL (Huijing *et al.* 1998, Maas *et al.* 2001). As EDL is distally lengthened, myofascial connections at the interface between TA + EHL and EDL lengthen and

forces generated by sarcomeres within the TA + EHL will be exerted on the distal EDL tendon.

Myofascial force transmission at lower firing frequencies

Although the absolute magnitude of EDL active force transmitted through epimuscular myofascial connections (i.e. the difference between distally and proximally measured forces) peaked at 100 Hz (Fig. 6a), the normalized force difference (proximo-distal force difference normalized for distal optimum force per frequency) was highest at 10 Hz (Fig. 6b). For TA + EHL active forces (Fig. 7), the normalized decrease in active force was also found to be enhanced at lower firing frequencies. This indicates that, as stimulation frequency decreases, a larger fraction of the force is transmitted via epimuscular myofascial connections. Apparently, as stimulation frequency was lowered, the stiffness of the myofascial pathways (not containing serial sarcomeres) decreased less than the stiffness of the sarcomeres in series – myotendinous pathway. The decreased stiffness of the serial sarcomeres, which affected our results in a major way, is a function of the decreased number of cross-bridges binding to actin filaments. In fully dissected rat muscles it was found that for each stimulation frequency, a typical force stiffness curve existed (Ettema & Huijing 1994), indicating a lower serial stiffness for sarcomeres – myotendinous pathway at lower forces.

Effects of stimulation frequency on length–force characteristics

The dependence of length–force characteristics on stimulation frequency is a well-known phenomenon for fully dissected muscle since the observations of Rack & Westbury (1969). For fully dissected muscles at submaximal levels of stimulation, shifts in muscle optimum length arise from the length-dependent Ca-sensitivity of force (Rack & Westbury 1969, Stephenson & Wendt 1984). At sarcomere lengths higher than optimum length of maximal activation, the effects of decreased filament overlap are counteracted by a higher force exerted per unit $[Ca^{2+}]$. These two counteracting effects create new optimal conditions for active force at higher lengths. The use of both synchronous stimulation as well as a distributed stimulation of groups of motor units at variable stimulation frequencies by Rack & Westbury (1969) showed that at low firing frequencies, a distributed stimulation protocol provides smoother tetani than synchronous stimulation, and is thus one step closer to physiological conditions. However, the firing frequency dependence of length–force characteristics still holds true during synchronous stimulation (Mela *et al.* 2002). In addition

to shifts in muscle optimum lengths, muscle active slack length was found to shift to higher muscle lengths as firing frequency is decreased (Rack & Westbury 1969, Roszek & Huijing 1997, Brown *et al.* 1999).

Effects of myofascial force transmission on firing frequency-related shifts in optimum muscle length

In accordance with results of Rack & Westbury (1969; for fully dissected cat soleus muscle), Brown *et al.* (1999; for dissected feline caudofemoralis muscle), and Roszek & Huijing (1997; for fully dissected rat GM muscle), our present results show that also for a muscle within an intact compartment, lower stimulation frequencies are always accompanied by a progressive shift of optimum EDL length to higher lengths (Fig. 5). However, this shift is not equal for distally and proximally measured forces (Fig. 5b), indicating effects of additional factors.

It should be noted, however, that optimum length cannot be measured directly, since only passive force and total force is measured experimentally. As active force is calculated by subtracting passive force before or after the tetanic contraction from total force, only an estimate of optimum length for whole muscle is obtained (MacIntosh & MacNaughton 2005). Therefore, the actual shifts in optimum lengths will be enhanced compared with our present results; passive force becomes relatively more important at higher muscle lengths and the underestimation of optimum length will increase.

In fully dissected and maximally activated muscle the following additional factors determine muscle optimum length (length of maximal active force exertion): (1) effects of pennation; (2) elastic effects of series elastic structures; and (3) the serial distribution in sarcomere lengths.

For muscles within its *in vivo* context of connective tissues, this reasoning has to be extended to include effects of an enhanced parallel distribution of sarcomeres lengths [or fibre mean sarcomeres length (Huijing 1996)], distinguishing proximal and distal fibre populations of muscle fibres within the muscle. Finite element modelling of muscle with connections to the extracellular matrix (Yucesoy *et al.* 2003) shows that substantial differences in fibre mean sarcomere lengths are to be expected between proximal and distal parts of the muscle, which are affected by asymmetries of muscle geometry and asymmetries of stiffness of myofascial connections.

Our present results also provide indirect evidence for the presence of a serial distribution of sarcomeres lengths within muscle fibres: near optimum lengths (Figs 3 and 5a) absolute EDL active force exerted at the distal tendon is higher than at the proximal tendon.

There are two, mutually exclusive, alternative explanations for this phenomenon:

- (1) Individual sarcomeres within the distal segment of EDL muscle fibres are active on the descending limb of their length force curves. Therefore, if they exert higher active forces, they would be active at lower lengths than the proximal sarcomeres within the same fibres. In accordance with results of (Julian & Morgan 1979), who related directly measured sarcomeres dynamics to the duration of creep, the enhanced creep in the proximal force traces (Fig. 3) would indicate the increased sarcomeres dynamics within muscle fibres at higher lengths. In such a case, the lower optimum length found for proximal EDL at 10 and 100 Hz firing frequencies would be explained by such serial distribution of sarcomeres length.
- (2) Individual sarcomeres within the distal segment of EDL muscle fibres are active on the ascending limb of their length force curves. Therefore, they would be active at higher lengths than the proximal sarcomeres within the same fibres. This view is supported by finite element model results that explained well the principle of epimuscular myofascial force transmission and its experimentally found effects on muscle length force characteristics (Yucesoy *et al.* 2003).

To discriminate between these two alternative explanations the following arguments are used: (1) On activation, the degree of shortening of sarcomeres is determined by the compliance of the series elastic elements. Within single muscle fibres (Julian & Morgan 1979), serial sarcomeres and their myotendinous connections and thus intersarcomere dynamics are the determining factor because of the comparatively low stiffness of the (remnants of) endomysium. In contrast for sarcomeres of a muscle acting within its *in vivo* context of connective tissues, the length and compliance series elastic components (serial sarcomeres and remnants of the endomysium) are not affected predominantly by the sarcomeres of the muscle fibre considered, but also by sarcomeres as well as connected endo- and perimysial stromata of muscle fibres adjacent with in the muscle (and given epimuscular myofascial force transmission even by more distant structures). In such a case, additional forces are exerted on the myofascial series elastic elements. Consequently, these series elastic elements are expected to be at higher lengths and thus stiffer and stable equilibrium sarcomere lengths are expected to be attained faster than in single muscle fibres (Yucesoy *et al.* 2003). These authors showed that the experimentally determined creep duration showed no direct relation to the calculated serial distribution of fibre strain (being an estimate for sarcomeres length). In

contrast to single fibre results, high equilibrium serial distributions would be preceded by low creep durations. (2) For the passive muscle a higher force is indicative of higher sarcomere lengths. This means that, prior to stimulation at different frequencies, the distal sarcomeres within muscle fibres of EDL are at higher lengths than their proximal counterparts. In such conditions, a reversal of serial sarcomeres length distribution upon activation is highly unlikely as the shorter proximal sarcomeres within EDL muscle fibres would be exposed to more compliant series elastic elements and would shorten more than their distal counterparts.

Therefore, we conclude that the second explanation is the more likely one: near optimum lengths, distal sarcomeres attain a higher length than the proximal ones within the same muscle fibres.

If for all muscle fibres of EDL the same serial distribution of sarcomeres length would be present, for all firing frequencies one would expect distally determined EDL optimal force to occur at lower muscle lengths than proximally determined EDL optimal force. However, our present results indicate either no effect (Fig. 5b: 20 and 30 Hz) or an opposite effect (Fig. 5b: 10 Hz). Therefore, we hypothesize that a parallel distribution of fibre mean sarcomeres length, enhanced by epimuscular myofascial force transmission caused net differences between proximally and distally determined optimum muscle lengths (at 10 and 100 Hz) and just compensated opposing effects at intermediate firing frequencies. This happens because additional forces transmitted via epimuscular connections are not exerted equally on all muscle fibres. For example, the neurovascular tract giving off branches of nerves and blood vessels to the muscles while coursing through the compartment in distal direction becomes smaller in diameter and less stiff.

Effects of myofascial force transmission on frequency-related shifts in active slack lengths

In contrast to the findings on fully dissected muscle (Rack & Westbury 1969, Roszek & Huijing 1997, Brown *et al.* 1999) in which a lowered firing frequency shifted muscle active slack length progressively to higher muscle lengths, no significant firing frequency related shifts of distal active slack length were found in our current study (Fig. 4a).

Muscle active slack length is the muscle length at which no active force is exerted by sarcomeres within a fibre on structures outside of the muscle. Therefore, muscle active slack length is not attained until the last sarcomere exerting force did shorten to its active slack length. In addition to elastic and pennation effects, serial or parallel distributions of sarcomere lengths may affect the muscle length at which this condition is

fulfilled. Firing frequency-related shifts of active slack length in fully dissected muscles are thought to be due to intracellular mechanisms related to the lower sensitivity to calcium at lower lengths (Rack & Westbury 1969, Roszek & Huijing 1997, Brown *et al.* 1999). Therefore, one would expect a shift in active slack length to be present also for a muscle within an intact compartment, unless a compensating effect is created by the presence of such myofascial connections. Such a compensation of a shift in active slack length is not likely to be the result of a serial distribution of sarcomere lengths; at lower firing frequencies, the serial distribution is negligible (ΔF EDL approaches zero). Therefore, it is hypothesized that at lower firing frequencies, the increased role of myofascial force transmission causes an increased parallel distribution in sarcomere lengths (i.e. enhanced distribution in fibre mean sarcomere lengths). In order to compensate the frequency-related shift in active slack length to higher muscle lengths, this increased parallel distribution should be characterized by an increased incidence of higher lengths of the sarcomeres still exerting force at low muscle lengths.

In conclusion, epimuscular myofascial force transmission becomes increasingly important at low stimulation frequencies, indicating that the relative stiffness of the serial sarcomeres-myotendinous path decreased more than that of the myofascial paths. The firing frequency dependent effects on length–force characteristics are modified by myofascial force transmission and create different effects at opposite ends of the muscle. Such effects should be taken into account for muscles operating within their *in vivo* context of connective tissues. Changes of distributions of sarcomere lengths (particularly parallel distributions) are hypothesized to play a major role in these effects.

Contributions by anonymous reviewers of this Journal pointing out the first of the alternatives for serial sarcomere length distribution are gratefully acknowledged.

Conflict of interest

The authors declare that they have no conflict of interest.

References

Brown, I.E., Cheng, E.J. & Loeb, G.E. 1999. Measured and modeled properties of mammalian skeletal muscle. II. The effects of stimulus frequency on force–length and force–velocity relationships. *J Muscle Res Cell Motil* 20, 627–643.

Ettema, G.J. & Huijing, P.A. 1994. Frequency response to rat gastrocnemius medialis in small amplitude vibrations. *J Biomech* 27, 1015–1022.

Hennig, R. & Lomo, T. 1985. Firing patterns of motor units in normal rats. *Nature* 314, 164–166.

Huijing, P.A. 1996. Important experimental factors for skeletal muscle modelling: non-linear changes of muscle length force characteristics as a function of degree of activity. *Eur J Morphol* 34, 47–54.

Huijing, P.A. 1998. Muscle, the motor of movement: properties in function, experiment and modelling. *J Electromyogr Kinesiol* 8, 61–77.

Huijing, P.A. 2003. Muscular force transmission necessitates a multilevel integrative approach to the analysis of function of skeletal muscle. *Exerc Sport Sci Rev* 31, 167–175.

Huijing, P.A. & Baan, G.C. 2001a. Myofascial force transmission causes interaction between adjacent muscles and connective tissue: effects of blunt dissection and compartmental fasciotomy on length force characteristics of rat extensor digitorum longus muscle. *Arch Physiol Biochem* 109, 97–109.

Huijing, P.A. & Baan, G.C. 2001b. Extramuscular myofascial force transmission within the rat anterior tibial compartment: proximo-distal differences in muscle force. *Acta Physiol Scand* 173, 297–311.

Huijing, P.A. & Baan, G.C. 2003. Myofascial force transmission: muscle relative position and length determine agonist and synergist muscle force. *J Appl Physiol* 94, 1092–1107.

Huijing, P.A. & Jaspers, R.T. 2005. Adaptation of muscle size and myofascial force transmission: a review and some new experimental results. *Scand J Med Sci Sports* 15, 349–380.

Huijing, P.A., Baan, G.C. & Rebel, G.T. 1998. Non-myotendinous force transmission in rat extensor digitorum longus muscle. *J Exp Biol* 201, 682–691.

Julian, F.J. & Morgan, D.L. 1979. Intersarcomere dynamics during fixed-end tetanic contractions of frog muscle fibres. *J Physiol* 293, 365–378.

Kreulen, M., Smeulders, M.J., Hage, J.J. & Huijing, P.A. 2003. Biomechanical effects of dissecting flexor carpi ulnaris. *J Bone Joint Surg Br* 85, 856–859.

Kreulen, M., Smeulders, M.J. & Hage, J.J. 2004. Restored flexor carpi ulnaris function after mere tenotomy explains the recurrence of spastic wrist deformity. *Clin Biomech (Bristol, Avon)* 19, 429–432.

Kronecker, H. & Cash, T. 1880. Ueber die Beweglichkeit der Muskeln in ihrem natürlichen Zusammenhange. *Arch Physiol, Physiologische Abteilung Arch Anatomie Physiol*, 179–180.

Maas, H., Baan, G.C. & Huijing, P.A. 2001. Intermuscular interaction via myofascial force transmission: effects of tibialis anterior and extensor hallucis longus length on force transmission from rat extensor digitorum longus muscle. *J Biomech* 34, 927–940.

Maas, H., Baan, G.C., Huijing, P.A., Yucesoy, C.A., Koopman, B.H. & Grootenboer, H.J. 2003a. The relative position of EDL muscle affects the length of sarcomeres within muscle fibers: experimental results and finite-element modeling. *J Biomech Eng* 125, 745–753.

Maas, H., Yucesoy, C.A., Baan, G.C. & Huijing, P.A. 2003b. Implications of muscle relative position as a co-determinant of isometric muscle force: a review and some experimental results. *J Mech Med Biol* 3, 145–168.

MacIntosh, B.R. & MacNaughton, M.B. 2005. The length-dependence of muscle active force: considerations for parallel elastic properties. *J Appl Physiol* 98, 1666–1673.

- Mela, P., Veltink, P.H., Huijting, P.A., Salmons, S. & Jarvis, J.C. 2002. The optimal stimulation pattern for skeletal muscle is dependent on muscle length. *IEEE Trans Neural Syst Rehabil Eng* 10, 85–93.
- Rack, P.M. & Westbury, D.R. 1969. The effects of length and stimulus rate on tension in the isometric cat soleus muscle. *J Physiol (Lond)* 204, 443–460.
- Rijkelijkhuisen, J.M., Baan, G.C., de Haan, A., de Ruyter, C.J. & Huijting, P.A. 2005. Extramuscular myofascial force transmission for in situ rat medial gastrocnemius and plantaris muscles in progressive stages of dissection. *J Exp Biol* 208, 129–140.
- Roszek, B. & Huijting, P.A. 1997. Stimulation frequency history alters length–force characteristics of fully recruited rat muscle. *J Electromyogr Kinesiol* 7, 161–177.
- Smeulders, M.J., Kreulen, M., Hage, J.J., Baan, G.C. & Huijting, P.A. 2002. Progressive surgical dissection for tendon transposition affects length–force characteristics of rat flexor carpi ulnaris muscle. *J Orthop Res* 20, 863–868.
- Stephenson, D.G. & Wendt, I.R. 1984. Length dependence of changes in sarcoplasmic calcium concentration and myofibrillar calcium sensitivity in striated muscle fibers. *J Muscle Res Cell Motil* 5, 243–272.
- Stephenson, D.G. & Williams, D.A. 1982. Effects of sarcomere length on the force–pCa relation in fast- and slow-twitch skinned muscle fibers from the rat. *J Physiol (Lond)* 333, 637–653.
- Street, S.F. 1983. Lateral transmission of tension in frog myofibers: a myofibrillar network and transverse cytoskeletal connections are possible transmitters. *J Cell Phys* 114, 346–364.
- Street, S.F. & Ramsey, R.W. 1965. Sarcolemma: transmitter of active tension in frog skeletal muscle. *Science* 149, 1379–1380.
- Tidball, J.G. 1991. Force transmission across muscle cell membranes. *J Biomech* 24 (Suppl. 1), 43–52.
- Trotter, J.A. 2002. Structure-function considerations of muscle–tendon junctions. *Comp Biochem Physiol A Mol Integr Physiol* 133, 1127–1133.
- Trotter, J.A., Hsi, K., Samora, A. & Wofsy, C. 1985. A morphometric analysis of the muscle–tendon junction. *Anat Rec* 213, 26–32.
- Yucesoy, C.A., Koopman, B.H., Huijting, P.A. & Grootenboer, H.J. 2002. Three-dimensional finite element modeling of skeletal muscle using a two-domain approach: linked fiber-matrix mesh model. *J Biomech* 35, 1253–1262.
- Yucesoy, C.A., Koopman, B.H., Baan, G.C., Grootenboer, H.J. & Huijting, P.A. 2003. Effects of inter- and extramuscular myofascial force transmission on adjacent synergistic muscles: assessment by experiments and finite-element modeling. *J Biomech* 36, 1797–1811.